Elastic α-^{12}C scattering at low energies with the bound states of ^{16}O in effective field theory

Shung-Ichi Ando*
School of Mechanical and ICT Convergence Engineering, Sunmoon University, Asan, Chungnam 31460, Republic of Korea

(Received 20 July 2017; revised manuscript received 23 September 2017; published 12 January 2018)

The elastic α-^{12}C scattering for $l = 0,1,2,3$ channels at low energies is studied, including the energies of excited bound states of ^{16}O, in effective field theory. A new renormalization method is introduced due to the large suppression factor produced by the Coulomb interaction when the effective range parameters are fitted to the phase sift data. After fitting the parameters, the asymptotic normalization constants of the 0_2^+, 1_1^-, 2_1^+, 3_1^- states of ^{16}O are calculated. The uncertainties when the amplitudes are interpolated to the stellar energy region of the ^{12}C$(\alpha,\gamma)^{16}$O reaction are also discussed.

DOI: 10.1103/PhysRevC.97.014604

I. INTRODUCTION

The radiative α capture on carbon-12, ^{12}C$(\alpha,\gamma)^{16}$O, is one of the fundamental reactions in nuclear astrophysics, which determines the C/O ratio synthesized in the stars [1]. The reaction rate of the process at the Gamow peak energy, $T_G = 0.3$ MeV, however, cannot be determined in experiment due to the Coulomb barrier. It is necessary to employ a theoretical model to extrapolate the reaction rate down to T_G by fitting model parameters to experimental data typically measured at a few MeV. Since the 1960s, a lot of experimental and theoretical studies for the reaction have been carried out. See Refs. [2–5] for review.

The elastic α-^{12}C scattering at low energies is an important reaction to fix some parameters of a model for the study. Accurate measurements of the elastic scattering have been reported in Refs. [6,7], and those data provide indispensable input for the parameter fittings. Elastic-scattering data at low energies in general can be used for deducing an asymptotic normalization constant (ANC), which determines an overall strength of a nuclear reaction involving bound states [8–10].

The ANC of deuteron, for example, where the deuteron is a simple system consisting of loosely bound proton and neutron, leads to an overall factor of the reactions at low energies, such as radiative neutron capture on a proton at BBN energies [11,12] and proton-proton fusion in the Sun [13–16]. The ANC of deuteron is accurately determined by two effective range parameters: the deuteron binding momentum and effective range [17,18], which are accurately fixed from the deuteron binding energy and elastic NN scattering at low energies. On the other hand, to deduce ANCs for nuclear reactions relevant in nuclear-astrophysics is not so simple: The Coulomb interaction between heavier nuclei plays a negative role by preventing ones from obtaining elastic-scattering data at very low energies, which makes the deduction of ANCs in terms of effective range expansion difficult [19,20]. Recently, a new method of the parametrization for deducting the ANCs of nuclear reactions is suggested by Ramirez Suarez and Sparenberg [21], and new results of the ANCs by using the new method are reported in Refs. [22,23].

Effective field theories (EFTs) provide us a model independent and systematic method for theoretical calculations. An EFT for a system in question can be built by introducing a scale which separates relevant degrees of freedom at low energies from irrelevant degrees of freedom at high energies. An effective Lagrangian is written down in terms of the relevant degrees of freedom and perturbatively expanded by counting the number of derivatives order by order. The irrelevant degrees of freedom are integrated out and their effect is embedded in coefficients appearing in the Lagrangian. Thus, a transition amplitude is systematically calculated by writing down Feynman diagrams, while the coefficients appearing in the Lagrangian are fixed by experiment. For review, one may refer to Refs. [24–27]. Since the mid-1990s, various processes essential in nuclear-astrophysics have been investigated by constructing EFTs, which are $p(n,\gamma)d$ at BBN energies [11,12] and pp fusion [13–16], ^{3}He$(\alpha,\gamma)^7$Be [28], and ^{7}Be$(p,\gamma)^7$B [29,30] in the Sun.

In the previous work [31], I have constructed an EFT of the radiative capture reaction, ^{12}C$(\alpha,\gamma)^{16}$O, obtained the counting rules for the reaction at T_G and fitted some parameters of the theory to the phase-shift data of the elastic scattering. (I briefly review the counting rules for the radiative capture and elastic-scattering reactions in the following sections.) In the parameter fitting to the phase-shift data, I have introduced resonance energies of ^{16}O as a large scale of the theory. As suggested by Teichmann [32], below the resonance energies, the Breit-Wigner-type parametrization for resonances can be expanded in powers of the energy, and one can obtain an expression of the amplitude in terms of the effective range expansion. I have determined three effective range parameters of the elastic scattering for $l = 0,1,2$ channels by fitting them to the phase-shift data but not included the excited bound states of ^{16}O in the study. Though the phase-shift data below the resonance energies can be reproduced very well by using the fitted parameters, I find that significant uncertainties in the elastic amplitudes are remained when extrapolating them to T_G.

In the present work, I incorporate the excited binding energies for 0_2^+, 1_1^-, 2_1^+, 3_1^- ($l^\pi_{i\text{th}}$) states of ^{16}O in the parameter

*sando@sunmoon.ac.kr

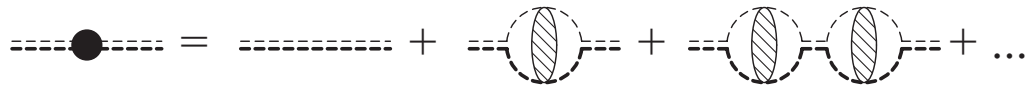

FIG. 1. Diagrams for dressed ^{16}O propagator. A thick (thin) dashed line represents a propagator of ^{12}C (α), and a thick and thin double dashed line with and without a filled blob represent a dressed and bare ^{16}O propagator, respectively. A shaded blob represents a set of diagrams consisting of all possible one-potential-photon-exchange diagrams up to infinite order and no potential-photon-exchange one.

fitting to the phase-shift data of the elastic scattering for $l = 0,1,2,3$ channels. An assumption for the parameter fitting is that fitted curves which interpolate the amplitude between the phase-shift data and the excited binding energies can be represented by several terms of a polynomial function. As will be discussed in detail below, however, I find a mismatch between the strength of the amplitudes estimated from the phase-shift data and the first few terms of a polynomial function obtained from the Coulomb self-energy term in the dressed ^{16}O propagator. Because those terms from the Coulomb self-energy are larger, at most by two orders of magnitude, than the term estimated by the phase-shift data, I introduce a new renormalization method; I assume that those large terms should be renormalized by counter terms, the role of which I assign to the effective range terms. Thus I include the effective range parameters up to third order ($n = 3$ in powers of k^{2n}) for the $l = 0,1,2$ channels and up to fourth order ($n = 4$) for the $l = 3$ channel. After fitting the parameters to the phase-shift data, I calculate the ANCs of the 0^+_2, 1^-_1, 2^+_1, 3^-_1 states of ^{16}O and compare the results to the existing ones.

This paper is organized as follows: In Sec. 2, the approach based on an EFT for the radiative capture reaction is briefly reviewed, and the expression of equations related to the elastic-scattering amplitudes, the phase shifts, and the effective range parameters are displayed. In Sec. 3, I introduce a new renormalization method and describe the details of the numerical fitting to the elastic-scattering data. In Sec. 4, the numerical results obtained in this work are exhibited, and, finally, in Sec. 5, the results and discussion of the work are presented. In the Appendix, the structure of the UV divergence and the counter terms of the elastic-scattering amplitudes in the conventional renormalization method are summarized.

II. EFT FOR THE RADIATIVE CAPTURE AND ELASTIC SCATTERING AT LOW ENERGIES

In the study of the radiative capture process, ^{12}C$(\alpha,\gamma)^{16}$O, at $T_G = 0.3$ MeV employing an EFT, at such a low energy, one may regard the ground states of α and ^{12}C as pointlike particles, whereas the first excited state energies of α and ^{12}C are chosen as irrelevant degrees of freedom, by which a large scale of the theory is determined. The effective Lagrangian for the process is constructed in terms of two spinless scalar fields for α and ^{12}C, and the terms of the Lagrangian are expanded in terms of the number of derivatives. An expression of the effective Lagrangian has been obtained in Eq. (1) in Ref. [31]. The expansion parameter of the theory is $Q/\Lambda_H \sim 1/3$, where Q denotes a typical momentum scale $Q \sim k_G$: k_G is the Gamow peak momentum, $k_G = \sqrt{2\mu T_G} \simeq 41$ MeV, where μ is the reduced mass of α and ^{12}C. Λ_H denotes a large momentum scale $\Lambda_H \simeq \sqrt{2\mu_4 T_{(4)}}$ or $\sqrt{2\mu_{12} T_{(12)}} \sim 150$ MeV, where μ_4 is the reduced mass of one- and three-nucleon systems and μ_{12} is that of four- and eight-nucleon systems. $T_{(4)}$ and $T_{(12)}$ are the first excited energies of α and ^{12}C, respectively. By including the terms up to next-to-next-to-leading order, therefore, one may obtain about 10% theoretical uncertainty for the process.

The amplitudes of the elastic scattering are calculated from diagrams depicted in Figs. 1 and 2. In my previous works, I have obtained the scattering amplitudes for lth partial wave states as [31,33,34]

$$A_l = \frac{2\pi}{\mu}\frac{(2l+1)P_l(\cos\theta)e^{2i\sigma_l}W_l(\eta)C_\eta^2}{K_l(k) - 2\kappa H_l(k)}, \tag{1}$$

where k is the magnitude of relative momentum between α and ^{12}C and θ is the scattering angle in the center-of-mass frame. In addition, η is the Sommerfeld parameter, $\eta = \kappa/k$, where κ is the inverse of the Bohr radius, $\kappa = Z_2 Z_6 \mu\alpha$, and

$$C_\eta^2 = \frac{2\pi\eta}{e^{2\pi\eta}-1}, \quad W_l(\eta) = \frac{\kappa^{2l}}{(l!)^2}\prod_{n=0}^{l}\left(1+\frac{n^2}{\eta^2}\right),$$
$$H_l(k) = W_l(\eta)H(\eta), \tag{2}$$

with

$$H(\eta) = \psi(i\eta) + \frac{1}{2i\eta} - \ln(i\eta), \tag{3}$$

where $\psi(z)$ is the digamma function, $P_l(x)$ are the Legendre polynomials, and σ_l are the Coulomb phase shifts. When η goes to zero, the factor C_η^2 is normalized to one, whereas, when η becomes large, the Gamow factor, $P = \exp(-2\pi\eta)$, appears from the factor $C_\eta^2 \propto P$. Note that the function, $-2\kappa H_l(k)$, in the denominator of the amplitude is obtained from the Coulomb bubble diagram for the dressed propagator of ^{16}O in Fig. 1, and the factor, $e^{2i\sigma_l}W_l(\eta)C_\eta^2$, in the numerator is from the initial and final state Coulomb interactions between α and ^{12}C in Fig. 2.

The function $K_l(k)$ represents the interaction due to the short-range nuclear force (compared with the long-range Coulomb force), which is obtained in terms of the effective

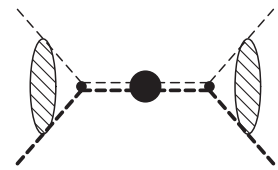

FIG. 2. Diagram of the scattering amplitude. See the caption of Fig. 1 as well.

range parameters as[1]

$$K_l(k) = -\frac{1}{a_l} + \frac{1}{2}r_l k^2 - \frac{1}{4}P_l k^4 + Q_l k^6 - R_l k^8 + \cdots . \quad (4)$$

Because the UV divergence comes out of the loop integrals in the Coulomb self-energy terms (from the diagrams in Fig. 1), one needs to introduce counter terms for renormalization. I employ the dimensional regularization and the structure of the UV divergence from the Coulomb self-energy terms is given in the Appendix. Thus, I need to include one counter term, $-1/a_0$ in the effective range expansion for $l = 0$; two counter terms, $-1/a_1$ and r_1, for $l = 1$; three counter terms, $-1/a_2$, r_2, and P_2, for $l = 2$; and four counter terms, $-1/a_3$, r_3, P_3, and Q_3 for $l = 3$ to remove the UV divergence and make the terms finite. The other higher-order terms in the effective range expansion are introduced as finite terms in the conventional renormalization method and supposed to obey counting rules in which higher-order terms are less important than lower-order terms. One can find that the expression obtained in Eq. (1) reproduces well the previous results reported in Refs. [19,37–39].

At the binding energies of excited states of ^{16}O, the amplitudes should have a pole at $k_b = i\gamma_l$, where γ_l are the binding momenta,[2] $\gamma_l = \sqrt{2\mu B_l}$; B_l denote the binding energies of excited states of ^{16}O. Thus the denominator of the scattering amplitude, $D_l(k)$, should vanish at k_b,

$$D_l(k_b) = K_l(k_b) - 2\kappa H_l(k_b) = 0\,. \quad (5)$$

Using this condition, the first effective range parameter, a_l, is related to other effective range parameters as

$$-\frac{1}{a_l} = \frac{1}{2}r_l\gamma_l^2 + \frac{1}{4}P_l\gamma_l^4 + Q_l\gamma_l^6 + R_l\gamma_l^8 + \cdots + 2\kappa H_l(k_b), \quad (6)$$

and I remove the a_l dependence from the amplitude. Thus, I have $D_l(k)$ as

$$D_l(k) = \tfrac{1}{2}r_l\left(k^2+\gamma_l^2\right) - \tfrac{1}{4}P_l\left(k^4-\gamma_l^4\right) + Q_l\left(k^6+\gamma_l^6\right) - R_l\left(k^8-\gamma_l^8\right) + \cdots - 2\kappa[H_l(k) - H_l(k_b)]. \quad (7)$$

The remaining effective range parameters are fixed by using the phase-shift data of the elastic scattering.

The differential cross section of the elastic scattering is represented in terms of the pure Coulomb scattering part and the Coulomb modified nuclear scattering part, as presented in Eq. (3) in Ref. [31], where the scattering function U_l is $U_l = \exp[2i(\delta_l + \omega_l)]$, where δ_l are the phase shifts for lth partial waves and $\omega_l = \sigma_l - \sigma_0$ with $\sigma_l = \arg\Gamma(1 + l + i\eta)$.

Thus the scattering amplitudes are represented in terms of δ_l as [40]

$$A_l = \frac{2\pi}{\mu}\frac{(2l+1)P_l(\cos\theta)e^{2i\sigma_l}}{k\cot\delta_l - ik}. \quad (8)$$

By comparing two expressions of the amplitudes A_l in Eqs. (1) and (8), one has a relation between the phase shift and the effective range parameters in $D_l(k)$ as

$$W_l(\eta)C_\eta^2 k\cot\delta_l = Re\,D_l(k). \quad (9)$$

To estimate the ANC, $|C_b|$, for the 0_2^+, 1_1^-, 2_1^+, 3_1^- states of ^{16}O, we employ the definition of $|C_b|$ from Eq. (14) in Ref. [39]:

$$|C_b| = \gamma_l^l\frac{\Gamma(l+1+|\eta_b|)}{l!}\left(\left|-\frac{dD_l(k)}{dk^2}\right|_{k^2=-\gamma_l^2}\right)^{-\frac{1}{2}} \quad (\mathrm{fm}^{-1/2}), \quad (10)$$

where $\eta_b = \kappa/k_b$.

III. FITTING THE PARAMETERS TO PHASE-SHIFT DATA

Four excited states of ^{16}O exist below the α-^{12}C threshold, which I include in the parameter fitting in the present study. The binding energies, $B_i(l^\pi)$, of the ith excited bound states of ^{16}O in l^π states from the α-^{12}C threshold energy are $B_1(0^+) = 1.113$, $B_2(3^-) = 1.032$, $B_3(2^+) = 0.245$, $B_4(1^-) = 0.045$ MeV. Thus, the binding momenta, $\gamma_l = \sqrt{2\mu B_i(l^\pi)}$, are

$$\gamma_l = 79.843,\ 15.860,\ 37.007,\ 75.954 \quad (\mathrm{MeV}), \quad (11)$$

for the 0_2^+, 1_1^-, 2_1^+, 3_1^- states, respectively, where $\mu = m_\alpha m_C/(m_\alpha + m_C) = 2795.079$ MeV with $m_\alpha = 3727.379$ MeV and $m_C = 11174.862$ MeV. As mentioned above, the first effective range term, a_l, is constrained by using the binding momenta.

To fix the other effective range parameters, the phase-shift data for each lth partial wave state are used. In the present work, I employ the phase-shift data from Tischhauser *et al.*'s paper [7]. The reported energies of the α particle in the laboratory frame are $T_\alpha = 2.6$–6.6 MeV, and corresponding momenta in the center-of-mass frame are $k = 105$–166 MeV (i.e., $k = \sqrt{1.5\mu T_\alpha}$). Because our large momentum scale of the theory is $\Lambda_H \sim 150$ MeV, the convergence of the expansion series should be carefully examined when the elastic-scattering data are used for the parameter fitting. In addition, because I do not explicitly include the resonance states of ^{16}O in the theory, I restrict data sets for the parameter fitting below the resonance energies, $T_\alpha = 6.52, 3.23, 3.57, 5.09$ MeV for 0_3^+, 1_2^-, 2_2^+, 3_2^- states, respectively; the corresponding momenta are $k = 166$, 117, 123, 146 MeV for the $l = 0, 1, 2, 3$, channels, respectively. (I will mention data sets I choose for the parameter fitting in detail below.)

Now I am in position to discuss a new renormalization method. The effective range parameters in $K_l(k)$ are expanded in powers of k^2, whereas the real part of the function $H_l(k)$ can be expanded in powers of k^2 as well. For the function $H(\eta)$ in

[1] In this work, I employ a modified representation for effective range parameters from that presented in Ref. [35]. Here I use the effective volume-like parameter P_l rather than the shape parameter P_l represented as $-r_l^2 P_l k^4$. In addition, I introduced an opposite sign for the R_l term so as to have positive sign in the bounding energy in Eq. (6). I had employed another parametrization (v parametrization) for the effective range parameters in Ref. [36].

[2] The quantity γ_l is also referred to the bound-state wave number in the low-energy scattering theory.

$H_l(k)$, one has

$$ReH(\eta) = \frac{1}{12\kappa^2}k^2 + \frac{1}{120\kappa^4}k^4 + \frac{1}{252\kappa^6}k^6 + \frac{1}{240\kappa^8}k^8 + \cdots, \quad (12)$$

where $\eta = \kappa/k$; κ is the inverse of the Bohr radius, $\kappa \simeq 245$ MeV, and is regarded as another large scale of the theory. This expansion is reliable in the present study for the elastic scattering at low energies along with the effective range expansion in $K_l(k)$. Thus, the right-hand-side of equation, $ReD_l(k)$, in Eq. (9) can be expanded as a power series of k^2 for both $K_l(k)$ and $2\kappa ReH_l(k)$. Meanwhile, the left-hand side of Eq. (9) is suppressed by the factor C_η^2, due to the Gamow factor $P = \exp(-2\pi\eta)$.

In the case of the s wave, for example, the reported phase shift at the smallest energy, $T_\alpha = 2.6$ MeV, is $\delta_0 = -1.893^\circ$ [7]. The factor C_η^2 becomes $C_\eta^2 \simeq 6\times10^{-6}$ at $k = 104$ MeV which corresponds to $T_\alpha = 2.6$ MeV, and the left-hand side of Eq. (9) numerically becomes $C_\eta^2 k\cot\delta_0 = -0.019$ MeV. The function $2\kappa ReH_0(k)$ is expanded as

$$2\kappa ReH_0(k) = \frac{1}{6\kappa}k^2 + \frac{1}{60\kappa^3}k^4 + \frac{1}{126\kappa^5}k^6 + \frac{1}{120\kappa^7}k^8 + \cdots = 7.441 + 0.136 + 0.012 + 0.002 + \cdots \ (\text{MeV}), \quad (13)$$

at $k = 104$ MeV. The numerical values in the second line of Eq. (13) correspond to the terms appearing in the first line of the equation in order. One can see that the power series converges well, but the first and second terms are two and one order of magnitude larger compared with the value estimated by using the experimental data in the left-hand side of Eq. (9), -0.019 MeV. Thus, I regard those terms unnaturally large, and it is necessary to introduce a new renormalization method, in which the counter terms remove the unnaturally large terms and make the terms in a natural size. In other words, I assume that fitting polynomial functions are represented as a natural power series at the low-energy region, and to maintain such polynomial functions, large cancellations for the first and second terms with the r_l and P_l effective terms, respectively, are expected. So I include the three effective range parameters, r_l, P_l, and Q_l, for the $l = 0$ channel, as the counter terms. The same tendency can be seen in the $l = 1,2$ channels, whereas one needs four effective range parameters for the $l = 3$ channel. Thus, I employ the three effective range parameters, r_l, P_l, Q_l, for the $l = 0,1,2$ channels and the four effective range parameters, r_l, P_l, Q_l, R_l, for the $l = 3$ channel when fitting the parameters to the phase-shift data below.[3]

IV. NUMERICAL RESULTS

As discussed above, I fit the three effective range parameters, r_l, P_l, and Q_l, to the phase-shift data for the $l = 0,1,2$ channels and the four effective range parameters, r_l, P_l, Q_l, and R_l, to those for the $l = 3$ channel, while a_l are constrained by using the relation in Eq. (6) with the binding momenta γ_l. To examine the sensitivity to the choice of data sets, I employ three sets of the phase-shift data [7] below the resonance energy for each partial wave, which have different energy ranges: three data sets for $l = 0$ denoted by $S0$, $S1$, $S2$ have the data at $T_\alpha = 2.6$–3.6, 2.6–3.8, and 2.6–4.0 MeV, respectively; those for $l = 1(2)$ denoted by $P0$, $P1$, $P2$ ($D0$, $D1$, $D2$) have the data at $T_\alpha = 2.6$–3.0, 2.6–3.1, 2.6–3.2 MeV, respectively; and those for $l = 3$ denoted by $F0$, $F1$, $F2$ have the data at $T_\alpha = 2.6$–4.6, 2.6–4.8, 2.6–5.0 MeV, respectively.

When the parameters are fitted to the data, large cancellations between the terms in powers of k^2 appearing from the $K_l(k)$ and $2\kappa H_l(k)$ functions, the r_l, P_l, Q_l, R_l effective range terms and the corresponding terms from the $2\kappa H_l(k)$ function are expected. I denote the terms from the $2\kappa H_l(k)$ function corresponding to the effective range terms as $\tilde r_l$, $\tilde P_l$, $\tilde Q_l$, $\tilde R_l$, and I have

$$\tilde r_0 = \frac{1}{3\kappa}, \quad \tilde P_0 = -\frac{1}{15\kappa^3}, \quad \tilde Q_0 = \frac{1}{126\kappa^5}, \quad (14)$$

$$\tilde r_1 = \frac{1}{3}\kappa, \quad \tilde P_1 = -\frac{11}{15\kappa}, \quad \tilde Q_1 = \frac{31}{1260\kappa^3}, \quad (15)$$

$$\tilde r_2 = \frac{1}{12}\kappa^3, \quad \tilde P_2 = -\frac{51}{60}\kappa, \quad \tilde Q_2 = \frac{191}{1008\kappa}, \quad (16)$$

$$\tilde r_3 = \frac{1}{108}\kappa^5, \quad \tilde P_3 = -\frac{47}{180}\kappa^3, \quad \tilde Q_3 = \frac{5297}{22680}\kappa, \quad \tilde R_3 = -\frac{17101}{90720\kappa}. \quad (17)$$

[3] In the new method of the parametrization of elastic scattering suggested by Ramirez Suarez and Sparenberg, the $K_l(k)$ and $2\kappa H_l(k)$ functions are merged, and a new function for the parametrization is defined as $\Delta_l(E) = C_\eta^2 k\cot\delta_l$, which is parameterized by using the Pade approximation [21].

TABLE I. Effective range parameters, r_0, P_0, Q_0, fitted by using the data sets $S0$, $S1$, $S2$; values of $\tilde r_0$, $\tilde P_0$, $\tilde Q_0$ are included in the last row. The values of a_0, ReD_{0G}, and $|C_b|$ for the 0_2^+ state are calculated by using r_0, P_0, Q_0. For details, see the text.

	a_0 (fm)	r_0 (fm)	P_0 (fm^3)	Q_0 (fm^5)	ReD_{0G} (MeV)	$\lvert C_b\rvert$ (fm$^{-1/2}$)
$S0$	6.2×10^4	0.268514(3)	$-0.0343(4)$	0.0019(2)	$4.2(7)\times10^{-3}$	$6.8(16)\times10^2$
$S1$	6.6×10^4	0.268514(3)	$-0.0342(3)$	0.0020(3)	$4.0(5)\times10^{-3}$	$7.4(15)\times10^2$
$S2$	5.8×10^4	0.268513(3)	$-0.0345(2)$	0.0018(1)	$4.4(4)\times10^{-3}$	$6.4(7)\times10^2$
	–	$\tilde r_0$ (fm)	$\tilde P_0$ (fm^3)	$\tilde Q_0$ (fm^5)	–	–
	–	0.268735	-0.0349	0.0027	–	–

TABLE II. Effective range parameters, r_1, P_1, Q_1, fitted by using the data sets $P0$, $P1$, $P2$; values of $\tilde{r}_1$, $\tilde{P}_1$, $\tilde{Q}_1$ are included in last row. The values of a_1, ReD_{1G}, and $|C_b|$ for the 1^-_1 state are calculated by using r_1, P_1, Q_1. For details, see the text.

	a_1(fm^3)	r_1 (fm^{-1})	P_1 (fm)	Q_1 (fm^3)	ReD_{1G} (MeV^3)	$\lvert C_b\rvert$ (fm$^{-1/2}$)
$P0$	-1.8×10^5	0.4150(6)	−0.577(8)	0.019(3)	$2.7(8)\times10^2$	$1.9(4)\times10^{14}$
$P1$	-1.6×10^5	0.4153(2)	−0.574(2)	0.020(1)	$3.0(3)\times10^2$	$1.8(1)\times10^{14}$
$P2$	-1.3×10^5	0.4157(2)	−0.569(2)	0.023(1)	$3.5(3)\times10^2$	$1.6(1)\times10^{14}$
	–	$\tilde{r}_1$ (fm^{-1})	$\tilde{P}_1$ (fm)	$\tilde{Q}_1$ (fm^3)	–	–
	–	0.4135	−0.591	0.013	–	–

Those values (and variations from them for some terms) are used as the initial input of the effective range parameters for the parameter fitting.[4]

In Tables I–IV, fitted values and errors of the effective range parameters, r_l, P_l, Q_l, R_l for $l=0,1,2,3$ channels to the data sets $\{S0,S1,S2\}$, $\{P0,P1,P2\}$, $\{D0,D1,D2\}$, and $\{F0,F1,F2\}$, respectively, are presented. The errors of the fitted parameters stem from those of the phase-shift data. Numerical values of the $\tilde{r}_l$, $\tilde{P}_l$, $\tilde{Q}_l$, $\tilde{R}_l$ terms for $l=0,1,2,3$ are also shown in the tables. The values of a_l are calculated by using the fitted effective range parameters in Eq. (6). The values in the second-to-last column are the real part of the denominator $ReD_l(k)$ of the scattering amplitude at the energy corresponding to T_G [5] (i.e., at $k=k_G$), and those in the last column are the ANC, $|C_b|$, for the 0^+_2, 1^-_1, 2^+_1, 3^-_1 states.

One can see that the errors of the fitted values of the effective range parameters are small, but the fitted effective range parameters are largely canceled with the corresponding $\tilde{r}_l$, $\tilde{P}_l$, $\tilde{Q}_l$, $\tilde{R}_l$ terms. In the values of the real part of denominator, ReD_{lG}, of the scattering amplitude at $k=k_G$, one finds significant errors: about 9–17%, 9–30%, 16–94%, 9–10% errors, depending on the choice of the data sets for the $l=0,1,2,3$ channels, respectively. A large uncertainty persists in the $l=2$ channel.

The ANCs for the 1^-_1 and 2^+_1 states have intensively been studied because those ANCs are related to the estimate of the $E1$ and $E2$ transitions of the radiative capture process, while those for the 0^+_2 and 3^-_1 states, which are also important to estimate the cascade transitions, are recently studied in experiment and reported first time.

For the ANC, $|C_b|$, for the 1^-_1 state, one finds that the result of the present study, $|C_b|=(1.6-1.9)\times10^{14}$ (fm$^{-1/2}$), is in good agreement with experimental values, $(2.10\pm0.14)\times10^{14}$, $(2.00\pm0.35)\times10^{14}$, and $(2.08\pm0.20)\times10^{14}$, obtained by Avila *et al.* [41], Oulebsir *et al.* [42], and Brune *et al.* [43], respectively, and underestimates for other experimental ones, $(5.1\pm0.6)\times10^{14}$ [44] and (17.4–26.4)$\times10^{14}$ [45]. One also finds good agreement with theoretical estimates, (2.22–2.24)$\times10^{14}$, obtained from a potential model calculation by Katsuma [46], and $2.14(6)\times10^{14}$ and 2.073×10^{14} from the new method of the parametrization by Ramirez Suarez and Sparenberg [21] and by Orlov *et al.* [23], respectively.

For the ANC, $|C_b|$, for the 2^+_1 state, the result of the present study, $|C_b|=(2.1$–$2.4)\times10^4$ (fm$^{-1/2}$), is in underestimates to experimental values, $(12.2\pm0.7)\times10^4$ [41], $(14.4\pm2.8)\times10^4$ [42], $(11\pm1)\times10^4$ [43], $(34.5\pm0.5)\times10^4$ [44], and (12.2–18.2)$\times10^4$ [45]. Other experimental estimates evaluated earlier, which basically agree with the experimental values mentioned above, can be found in Table VI in Ref. [47]. On the other hand, the result of the present study is in good agreement with theoretical estimates, $(2.41\pm0.38)\times10^4$ and 2.106×10^4, from the effective range analysis up to the r_2 term by Konig *et al.* [19] and up to the P_2 term by Orlov *et al.* [20], respectively, and in underestimates for the other theoretical estimates, $(14.45\pm0.85)\times10^4$ from the supersymmetric potential model by Sparenberg [48] and $(12.6\pm0.5)\times10^4$ from the R matrix analysis with a microscopic cluster model by Dufour and Descouvemont [47] and 5.050×10^4 from the new method of the parametrization by Orlov *et al.* [23].

For the ANCs, $|C_b|$, for the 0^+_2 and 3^-_1 states, the result of the present study, $|C_b|=(6.4$–$7.4)\times10^2$ (fm$^{-1/2}$) for the 0^+_2 state is in underestimate to an experimental value, $(15.6\pm1.0)\times10^2$ [41] and in overestimate to a theoretical value, 4.057×10^2 [23]. Meanwhile, the result of the present study, $|C_b|=(1.2-1.5)\times10^2$ (fm$^{-1/2}$) for the 3^-_1 state is in very good agreement with the experimental value, $(1.39\pm0.09)\times10^2$, recently reported by Avila *et al.* [41].

To examine the convergence of the power series in terms of k^2 at $k=k_G$, I add the effective range terms and those

[4] I employ a SciPy module, `curve_fit`, in optimization package when fitting the effective range parameters to the phase-shift data.

[5] The α energy in the laboratory frame corresponding to T_G is $T_\alpha=\frac{4}{3}T_G\simeq0.4$ MeV.

TABLE III. Effective range parameters, r_2, P_2, Q_2, fitted by using the data sets $D0$, $D1$, $D2$; values of $\tilde{r}_2$, $\tilde{P}_2$, $\tilde{Q}_2$ are included in the last row. The values of a_2, ReD_{2G}, and $|C_b|$ for the 2^+_1 state are calculated by using r_2, P_2, Q_2. For details, see the text.

	a_2(fm^5)	r_2 (fm^{-3})	P_2 (fm^{-1})	Q_2 (fm)	ReD_{2G} (fm^{-5})	$\lvert C_b\rvert$ (fm$^{-1/2}$)
$D0$	10.3×10^3	0.155(4)	− 1.12(7)	0.11(3)	$-1.66(156)\times10^{-4}$	$2.4(3)\times10^4$
$D1$	6.5×10^3	0.152(2)	− 1.16(4)	0.08(2)	$-2.6(9)\times10^{-4}$	$2.3(2)\times10^4$
$D2$	4.3×10^3	0.149(2)	− 1.21(3)	0.06(1)	$-3.8(6)\times10^{-4}$	$2.1(1)\times10^4$
	–	$\tilde{r}_2$ (fm^{-3})	$\tilde{P}_2$ (fm^{-1})	$\tilde{Q}_2$ (fm)	–	–
	–	0.159	− 1.05	0.15	–	–

TABLE IV. Effective range parameters, r_3, P_3, Q_3, R_3, fitted by using the data sets $F0$, $F1$, $F2$; values of $\tilde{r}_3$, $\tilde{P}_3$, $\tilde{Q}_3$, $\tilde{R}_3$ are included in the last row. The values of a_3, ReD_{3G}, and $|C_b|$ for the 3_1^- state are calculated by using r_3, P_3, Q_3, R_3. For details, see the text.

	a_3 (fm^7)	r_3 (fm^{-5})	P_3 (fm^{-3})	Q_3 (fm^{-1})	R_3 (fm)	ReD_{3G} (fm^{-7})	$\lvert C_b\rvert$ (fm$^{-1/2}$)
$F0$	-1.4×10^3	0.0319(1)	$-0.453(11)$	0.317(9)	$-0.141(8)$	$7.8(8)\times10^{-4}$	$1.2(1)\times10^2$
$F1$	-1.5×10^3	0.0320(1)	$-0.459(9)$	0.311(7)	$-0.146(6)$	$7.4(7)\times10^{-4}$	$1.3(1)\times10^2$
$F2$	-1.8×10^3	0.0322(1)	$-0.472(7)$	0.301(6)	$-0.156(5)$	$6.4(6)\times10^{-4}$	$1.5(1)\times10^2$
	–	$\tilde{r}_3$ (fm^{-5})	$\tilde{P}_3$ (fm^{-3})	$\tilde{Q}_3$ (fm^{-1})	$\tilde{R}_3$ (fm)	–	–
	–	0.0272	-0.498	0.290	-0.152	–	–

from the $2\kappa ReH_l(k)$ functions together. In Table V, I show the ratios of the terms after normalizing those terms by $-1/a_l$ for $l = 0,2,3$ and by $\frac{1}{2}(r_1 - \tilde{r}_1)k_G^2$ for $l = 1$ because of their dominance where the effective range parameters fitted by using the data sets $S2$, $P2$, $D2$, $F2$ are used. As discussed above, the expansion parameter at T_G is $Q \sim 1/3$, so the k_G^2, k_G^4, k_G^6 terms are expected to be a few tenths, a few hundredths, and a few thousandths to the leading-order terms, respectively. One finds good convergence of the power series for $l = 0,3$ at $k = k_G$. On the other hand, the $-1/a_1$ term is small compared to the $\frac{1}{2}(r_1 - \tilde{r}_1)k_G^2$ term for $l = 1$ and the $-1/a_2$ and $\frac{1}{2}(r_2 - \tilde{r}_2)k_G^2$ terms are comparable for $l = 2$, but the higher-order terms are well converged for $l = 1,2$, as expected by the counting rules of the theory.

In Figs. 3–6, the curves of phase shift δ_l [(a) panels] and the real part of denominator, $ReD_l(k)$, of the scattering amplitude [(b) panels] for $l = 0,1,2,3$, respectively, are plotted as functions of T_α by using the values of r_l, P_l, Q_l, R_l, which are fitted by using the data sets denoted by $\{S0,S1,S2\}$, $\{P0,P1,P2\}$, $\{D0,D1,D2\}$, and $\{F0,F1,F2\}$. Experimental data of the phase shift are also included in the figures. In addition, a filled box in the (b) panels represents the binding energy of the excited 0_2^+, 1_1^-, 2_1^+, or 3_1^- state in each of the figures.

One finds that the curves of δ_l plotted by using the different sets of the fitted parameters are in good agreement with each other and reproduce the experimental data within the errors, except for the large energy region, $T_\alpha = 3.0$–3.2 MeV for $l = 1$. One can see the significant separations of the curves of $ReD_l(k)$ at the interpolated energy region where the experimental data do not exist for the $l = 1,2,3$ channels, but the values of ReD_{lG} at $k = k_G$ (i.e., $T_\alpha = 0.4$ MeV) for the different sets of the parameters are still in good agreement within the errors, as seen in the tables.

TABLE V. Ratios of the terms in the power series to $-1/a_l$ for $l = 0,2,3$ and to $\frac{1}{2}(r_1 - \tilde{r}_1)k_G^2$ for $l = 1$ at $k = k_G$, where the effective range parameters fitted by using the data sets $S2$, $P2$, $D2$, $F2$ have been used.

	$\lvert -\frac{1}{a_l}\rvert$	$\lvert\frac{1}{2}(r_l - \tilde{r}_l)k_G^2\rvert$	$\lvert -\frac{1}{4}(P_l - \tilde{P}_l)k_G^4\rvert$	$\lvert(Q_l - \tilde{Q}_l)k_G^6\rvert$
$S2$	1	0.276	0.012	0.004
$P2$	0.154	1	0.215	0.016
$D2$	1	0.946	0.316	0.031
$F2$	1	0.195	0.023	0.002

V. RESULTS AND DISCUSSION

In the present work, I have fitted the effective range parameters to the phase-shift data of the elastic scattering for $l = 0,1,2,3$ below the resonance energies of ^{16}O in EFT. The excited binding energies of the 0_2^+, 1_1^-, 2_1^+, 3_1^- states of ^{16}O are also included in the parameter fitting. Because of a mismatch between the terms from the $2\kappa H_l(k)$ functions and a term obtained from the phase-shift data, I have introduced a new renormalization method: I assign the effective range terms as a role of the counter terms to obtain a natural power series for the fitting polynomial functions at the low-energy region. Thus, I have fitted three effective range parameters, r_l, P_l, Q_l, for $l = 0,1,2$ and four effective range parameters, r_l, P_l, Q_l, R_l, for $l = 3$ to the phase-shift data. (Those fitted values of the effective range parameters are used when I study the radiative capture reaction of α and ^{12}C in EFT in the future.) After fitting the effective range parameters, I have calculated the real part of the denominator, ReD_{lG}, of the scattering amplitude at the energy corresponding to T_G and the ANCs for the 0_2^+, 1_1^-, 2_1^+, 3_1^- states. In addition, I have interpolated and plotted the real part of the denominator of the scattering amplitude between the binding energy and the phase-shift data.

In fitting the effective range parameters for the all partial waves, one finds that the errors of the fitted effective range parameters are tiny, whereas the effective range terms are almost exactly canceled with the terms from the $2\kappa H_l(k)$ function. Thus, I obtain 9–94% errors in ReD_{lG} depending on the choice of the input data sets and partial waves, while the power series in terms of k_G^2 in $ReD_l(k)$ well converges at the energy corresponding to T_G, as expected by the counting rules of the theory. In the figures, though the curves of the phase shifts plotted by using the different sets of the parameters are in good agreement, those of $ReD_l(k)$ are significantly different in the interpolated region between the binding energies and the phase-shift data where no experimental data are available. Nonetheless, ReD_{lG} from the different sets of the parameters are still in good agreement within the error bars.

For the ANC, $|C_b|$, for the 1_1^- state, I find that the result of the present study is in good agreement with the other theoretical estimates and the recent experimental estimates. Thus, the estimates of $|C_b|$ for the 1_1^- state converge both theoretically and experimentally. For the ANC, $|C_b|$, for the 2_1^+ state, the result of the present study is in good agreement with the theoretical estimates based on the effective range expansion but it underestimates, by more than a factor of 5, compared with those of the other theories and the experiments. As seen in

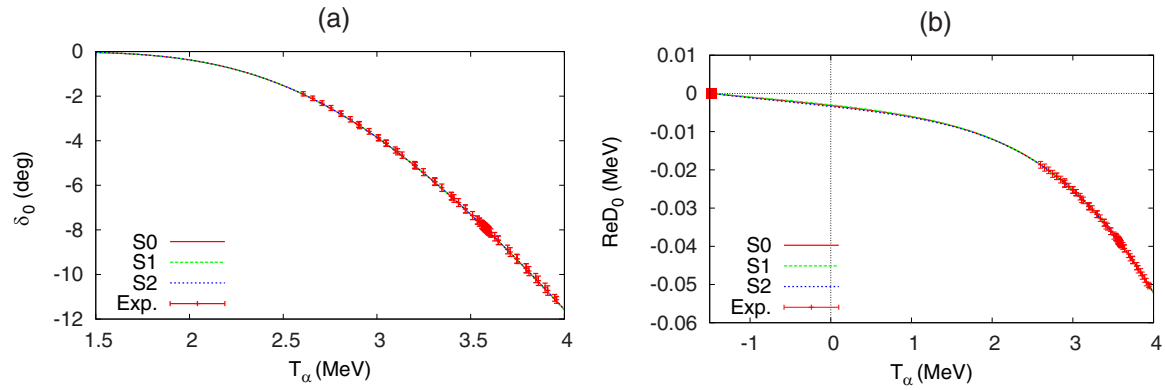

FIG. 3. Phase shift, δ_0, (a) and the real part of denominator, $ReD_0(k)$, of the amplitude (b) as functions of T_α (where $k = \sqrt{1.5\mu T_\alpha}$). Curves are plotted by using the effective range parameters, fitted from the $S0$, $S1$, $S2$ data sets, presented in Table I. Experiment phase-shift data are also included in the figure. A filled box in (b) represents the excited binding energy of the 0_2^+ state.

Eq. (10), such a large $|C_b|$ can be obtained by a very small slope of $ReD_2(k)$ at the binding energy of the 2_1^+ state. That indicates a very large scattering length and a drastic cancellation between the r_2 term and the $\tilde{r}_2$ term. Meanwhile, as seen in Fig. 5(b), the phase-shift data are quite distant from the bound-state energy, while the higher-order terms are involved in the fitting. Thus, it is hard to discriminate which curve is better than the others in the present approach. To have accurate experimental data of the phase shift down to, e.g., $T_\alpha = 1$ or 1.5 MeV could improve the situation. For the ANCs, $|C_b|$, for the 0_2^- and 3_1^- states, the first experimental result is recently reported by Avila *et al.* [41]. I find that the result for the 0_2^+ state is about half compared to the experimental estimate, while the result for the 3_1^- state is in good agreement with the experimental value. It may be necessary to wait for a further confirmation experimentally and theoretically for the 0_2^+ and 3_1^- states.

In the present work, I have introduced a new renormalization method from an observation of a mismatch between the terms from the Coulomb self-energy term, the $2\kappa H_l(k)$ function, and the term obtained from the phase-shift data by assuming to have a natural power series of the fitting polynomial functions at the low energies. A conjecture about the observation is, on one hand, that it may be caused simply due to the severe suppression factor, the Gamow factor, at the low energies. On the other hand, it may stem from the assumption that the α and ^{12}C states are pointlike. That implies that the interaction length scale between the α and ^{12}C vanishes, and thus the short-range effect should be renormalized by introducing the counter terms. A more systematic study about the issue would be necessary in the future.

ACKNOWLEDGMENTS

The author thanks J.-M. Sparenberg for helpful discussions. This work was supported by the Basic Science Research Program through the National Research Foundation of Korea funded by the Ministry of Education of Korea (Grant No. NRF-2016R1D1A1B03930122) and in part by the National Research Foundation of Korea (NRF) grant funded by the Korean government (Grant No. NRF-2016K1A3A7A09005580).

APPENDIX

In this Appendix, I display the UV divergent terms from the Coulomb self-energy in terms of the J functions and discuss the counterterms in the conventional renormalization method. The Coulomb self-energy terms for $l = 0,1,2,3$ are calculated

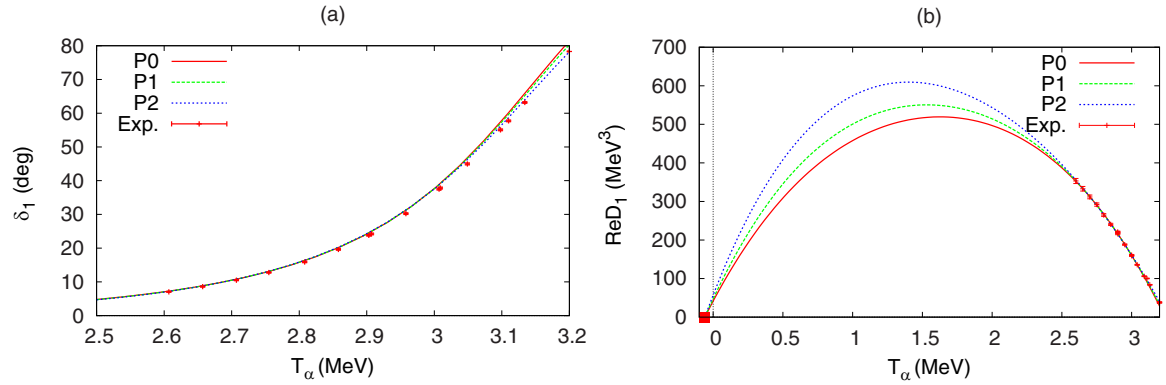

FIG. 4. Phase shift, δ_1, (a) and the real part of denominator, $ReD_1(k)$, of the amplitude (b) as functions of T_α. Curves are plotted by using the effective range parameters, fitted from the $P0$, $P1$, $P2$ data sets, presented in Table II. Experiment phase-shift data are also included in the figure. The filled box in (b) represents the binding energy of the 1_1^- state.

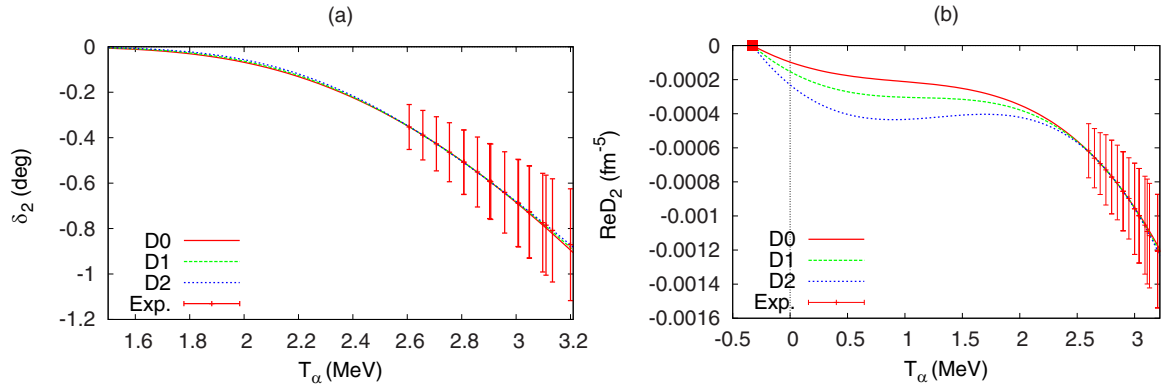

FIG. 5. Phase shift, δ_2, (a) and the real part of denominator, $ReD_2(k)$, of the amplitude (b) as functions of T_α. Curves are plotted by using the effective range parameters, fitted from the $D0$, $D1$, $D2$ data sets, presented in Table III. Experiment phase-shift data are also included in the figure. The filled box in (b) represents the binding energy of the 2_1^+ state.

from the J functions defined below:

$$J_0^{l=0}(p) = \int \frac{d^3\vec{q}}{(2\pi)^3}\frac{d^3\vec{q}'}{(2\pi)^3}\langle\vec{q}'|\hat{G}_C^{(+)}|\vec{q}\rangle, \tag{A1}$$

$$J_{2,i,x}^{l=1}(p) = \int \frac{d^3\vec{q}}{(2\pi)^3}\frac{d^3\vec{q}'}{(2\pi)^3} q_i'\langle\vec{q}'|\hat{G}_C^{(+)}|\vec{q}\rangle q_x, \tag{A2}$$

$$J_{4;ij,xy}^{l=2}(p) = \int \frac{d^3\vec{q}}{(2\pi)^3}\frac{d^3\vec{q}'}{(2\pi)^3}\left(q_i'q_j' - \frac{1}{3}\delta_{ij}q'^2\right) \times \langle\vec{q}'|\hat{G}_C^{(+)}|\vec{q}\rangle\left(q_xq_y - \frac{1}{3}\delta_{xy}q^2\right), \tag{A3}$$

$$J_{6,ijk,xyz}^{l=3}(p) = \int \frac{d^3\vec{q}}{(2\pi)^3}\frac{d^3\vec{q}'}{(2\pi)^3}\left[q_i'q_j'q_k' - \frac{1}{5}(\delta_{ij}q_k' + \delta_{ik}q_j' + \delta_{jk}q_i')q'^2\right]\langle\vec{q}'|\hat{G}_C^{(+)}|\vec{q}\rangle \times\left[q_xq_yq_z - \frac{1}{5}(\delta_{xy}q_z + \delta_{xz}q_y + \delta_{yz}q_x)q^2\right], \tag{A4}$$

where $\hat{G}_C^{(\pm)}$ is the Coulomb propagator, $G_C^{(\pm)} = 1/(E - \hat{H}_0 - \hat{V}_C \pm i\epsilon)$; $H_0 = \vec{p}^2/(2\mu)$ is the free two-particle Hamiltonian, μ is a reduced mass, and $V_C = \alpha Z_1 Z_2/r$ is the repulsive Coulomb force.

The J functions become infinity due to the loop integrals, and I employ the dimensional regularization in $d = 4 - 2\epsilon$ space-time dimensions. The expression of the $J_0^{l=0}(p)$ function is well known and one has [13]

$$J_0^{l=0}(p) = J_0^{l=0,\mathrm{div}} - \frac{\kappa\mu}{\pi}H(\eta), \tag{A5}$$

where $J_0^{l=0,\mathrm{div}}$ is the divergent part of the $J_0^{l=0}(p)$ function,

$$J_0^{l=0,\mathrm{div}} = \frac{\kappa\mu}{2\pi}\left[\frac{1}{\epsilon} - 3C_E + 2 + \ln\left(\frac{\pi\mu_{\mathrm{DR}}^2}{4\kappa^2}\right)\right], \tag{A6}$$

where $C_E = 0.577\cdots$ and μ_{DR} is a scale parameter from the dimensional regularization. In addition, $\kappa = \alpha Z_1 Z_2\mu$, and the $H(\eta)$ function has been presented in Eq. (3). I note that $J_0^{l=0,\mathrm{div}}$

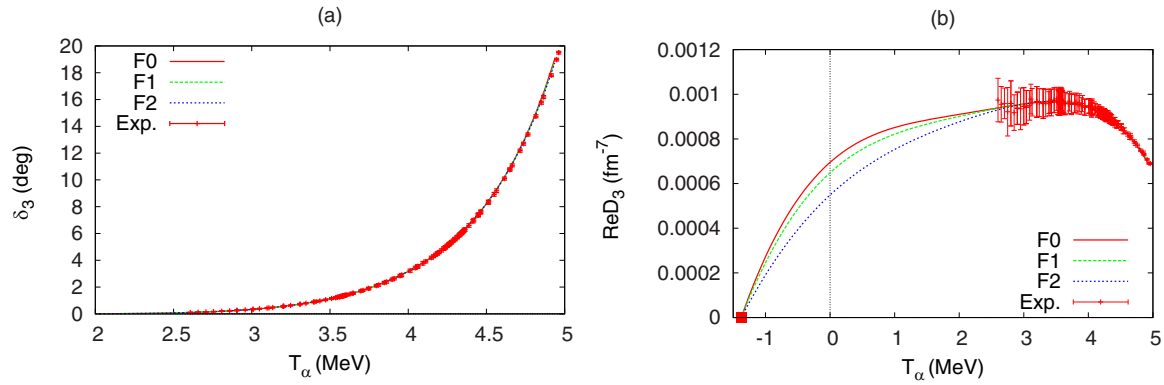

FIG. 6. Phase shift, δ_3, (a) and the real part of denominator, $ReD_3(k)$, of the amplitude (b) as functions of T_α. Curves are plotted by using the effective range parameters, fitted from the $F0$, $F1$ $F2$ data sets, presented in Table IV. Experiment phase-shift data are also included in the figure. The filled box in (b) represents the binding energy of the 3_1^- state.

does not depend on the momentum p. Thus the divergent term is renormalized by a counterterm, the $-1/a_0$ term in the effective range expansion for $l = 0$.

The UV divergent terms from the other J functions are obtained as

$$J^{l=1,\mathrm{div}}_{2,i,x}(p) = O^{l=1}_{i,x}(\kappa^2 + p^2) J^{l=0,\mathrm{div}}_0, \tag{A7}$$

$$J^{l=2,\mathrm{div}}_{4,ij,xy}(p) = O^{l=2}_{ij,xy}\tfrac{1}{4}(\kappa^2 + p^2)(\kappa^2 + 4p^2) J^{l=0,\mathrm{div}}_0, \tag{A8}$$

$$J^{l=3,\mathrm{div}}_{6,ijk,xyz}(p) = O^{l=3}_{ijk,xyz}\tfrac{1}{36}(\kappa^2 + p^2)(\kappa^2 + 4p^2) \times (\kappa^2 + 9p^2) J^{l=0,\mathrm{div}}_0, \tag{A9}$$

with

$$O^{l=1}_{i,x} = \int \frac{d\Omega_{\hat{l}}}{4\pi} \hat{l}_i \hat{l}_x = \frac{1}{3}\delta_{ix}, \tag{A10}$$

$$O^{l=2}_{ij,xy} = \int \frac{d\Omega_{\hat{l}}}{4\pi} \left(\hat{l}_i \hat{l}_j - \frac{1}{3}\delta_{ij}\right)\left(\hat{l}_x \hat{l}_y - \frac{1}{3}\delta_{xy}\right) = \frac{1}{15}\left(\delta_{ix}\delta_{jy} + \delta_{iy}\delta_{jx} - \frac{2}{3}\delta_{ij}\delta_{xy}\right), \tag{A11}$$

$$O^{l=3}_{ijk,xyz} = \int \frac{d\Omega_{\hat{l}}}{4\pi} \left[\hat{l}_i \hat{l}_j \hat{l}_k - \frac{1}{5}(\delta_{ij}\hat{l}_k + \delta_{ik}\hat{l}_j + \delta_{jk}\hat{l}_i)\right] \times \left[\hat{l}_x \hat{l}_y \hat{l}_z - \frac{1}{5}(\delta_{xy}\hat{l}_z + \delta_{xy}\hat{l}_y + \delta_{yz}\hat{l}_x)\right] = \frac{1}{105}\left[\delta_{ix}\delta_{jy}\delta_{kz} + 5 \text{ terms} - \frac{2}{5}(\delta_{ij}\delta_{kx}\delta_{yz} + 8 \text{ terms})\right]. \tag{A12}$$

To renormalize the divergent terms from the Coulomb self-energy, which now depend on the powers of p^2, one needs two counterterms, $-1/a_1$ and r_1, in the effective range expansion for $l = 1$, three counterterms, $-1/a_2$, r_2, and P_2, for $l = 2$, and four counterterms, $-1/a_3$, r_3, P_3, and Q_3, for $l = 3$.

[1] W. A. Fowler, Rev. Mod. Phys. **56**, 149 (1984).
[2] L. R. Buchmann and C. A. Barnes, Nucl. Phys. A **777**, 254 (2006).
[3] A. Coc, F. Hammache, and J. Kiener, Eur. Phys. J. A **51**, 34 (2015).
[4] C. A. Bertulani and T. Kajino, Prog. Part. Nucl. Phys. **89**, 56 (2016).
[5] R. J. deBoer *et al.*, Rev. Mod. Phys. **89**, 035007 (2017), references therein.
[6] R. Plaga *et al.*, Nucl. Phys. A **465**, 291 (1987).
[7] P. Tischhauser, A. Couture, R. Detwiler, J. Gorres, C. Ugalde, E. Stech, M. Wiescher, M. Heil, F. Kappeler, R. E. Azuma, and L. Buchmann, Phys. Rev. C **79**, 055803 (2009).
[8] A. M. Mukhamedzhanov and R. E. Tribble, Phys. Rev. C **59**, 3418 (1999).
[9] L. D. Blokhintsev and Y. O. Yeremenko, Phys. At. Nucl. **71**, 1219 (2008).
[10] R. E. Tribble *et al.*, Rep. Prog. Phys. **77**, 106901 (2014).
[11] G. Rupak, Nucl. Phys. A **678**, 405 (2000).
[12] S. Ando, R. H. Cyburt, S. W. Hong, and C. H. Hyun, Phys. Rev. C **74**, 025809 (2006).
[13] X. Kong and F. Ravndal, Nucl. Phys. A **656**, 421 (1999).
[14] M. Butler and J.-W. Chen, Phys. Lett. B **520**, 87 (2001).
[15] S. Ando, J. W. Shin, C. H. Hyun, S. W. Hong, and K. Kubodera, Phys. Lett. B **668**, 187 (2008).
[16] J.-W. Chen, C.-P. Liu, and S.-H. Yu, Phys. Lett. B **720**, 385 (2013).
[17] S. R. Beane and M. J. Savage, Nucl. Phys. A **694**, 511 (2001).
[18] S. I. Ando and C. H. Hyun, Phys. Rev. C **72**, 014008 (2005).
[19] S. Konig, D. Lee, and H.-W. Hammer, J. Phys. G: Nucl. Part. Phys. **40**, 045106 (2013).
[20] Yu. V. Orlov, B. F. Irgaziev, and L. I. Nikitina, Phys. Rev. C **93**, 014612 (2016).
[21] O. L. Ramirez Suarez, J.-M. Sparenberg, Phys. Rev. C **96**, 034601 (2017).
[22] L. D. Blokhintsev, A. S. Kadyrov, A. M. Mukhamedzhanov, and D. A. Savin, Phys. Rev. C **95**, 044618 (2017).
[23] Yu. V. Orlov, B. F. Irgaziev, and J.-U. Nabi, Phys. Rev. C **96**, 025809 (2017).
[24] P. F. Bedaque and U. van Kolck, Annu. Rev. Nucl. Part. Sci. **52**, 339 (2002).
[25] E. Braaten and H.-W. Hammer, Phys. Rep. **428**, 259 (2006).
[26] U.-G. Meißner, Phys. Scr. **91**, 033005 (2016).
[27] H.-W. Hammer, C. Ji, and D. R. Phillips, J. Phys. G: Nucl. Part. Phys. **44**, 103002 (2017).
[28] R. Higa, G. Rupak, and A. Vaghani, arXiv:1612.08959v1.
[29] X. Zhang, K. M. Nollett, and D. R. Phillips, Phys. Rev. C **89**, 051602(R) (2014).
[30] E. Ryberg, C. Forssen, H.-W. Hammer, and L. Platter, Eur. Phys. J. A **50**, 170 (2014).
[31] S.-I. Ando, Eur. Phys. J. A **52**, 130 (2016).
[32] T. Teichmann, Phys. Rev. **83**, 141 (1951).
[33] S. I. Ando, J. W. Shin, C. H. Hyun, and S. W. Hong, Phys. Rev. C **76**, 064001 (2007).
[34] S.-I. Ando, Eur. Phys. J. A **33**, 185 (2007).
[35] J.-M. Sparenberg, P. Capel, and D. Baye, J. Phys.: Conf. Ser. **312**, 082040 (2011).
[36] S.-I. Ando and C. H. Hyun, Phys. Rev. C **86**, 024002 (2012).
[37] J. Hamilton, I. Overbo, and B. Tromborg, Nucl. Phys. B **60**, 443 (1973).
[38] H. van Haeringen, J. Math. Phys. **18**, 927 (1977).
[39] J.-M. Sparenberg, P. Capel, and D. Baye, Phys. Rev. C **81**, 011601 (2010).
[40] A. M. Lane and R. G. Thomas, Rev. Mod. Phys. **30**, 257 (1957).
[41] M. L. Avila, G. V. Rogachev, E. Koshchiy, L. T. Baby, J. Belarge, K. W. Kemper, A. N. Kuchera, A. M. Mukhamedzhanov, D. Santiago-Gonzalez, and E. Uberseder, Phys. Rev. Lett. **114**, 071101 (2015).

[42] N. Oulebsir, F. Hammache, P. Roussel, M. G. Pellegriti, L. Audouin, D. Beaumel, A. Bouda, P. Descouvemont, S. Fortier, L. Gaudefroy, J. Kiener, A. Lefebvre-Schuhl, and V. Tatischeff, Phys. Rev. C **85**, 035804 (2012).
[43] C. R. Brune, W. H. Geist, R. W. Kavanagh, and K. D. Veal, Phys. Rev. Lett. **83**, 4025 (1999).
[44] A. Belhout *et al.*, Nucl. Phys. A **793**, 178 (2007).
[45] S. Adhikari and C. Basu, Phys. Lett. B **704**, 308 (2011).
[46] M. Katsuma, Phys. Rev. C **78**, 034606 (2008).
[47] M. Dufour and P. Descouvemont, Phys. Rev. C **78**, 015808 (2008).
[48] J.-M. Sparenberg, Phys. Rev. C **69**, 034601 (2004).